Electronic Supplementary Material (ESI) for RSC Advances.

Supporting Information

Easy synthesis of layered titanate nanosheets with 3D hierarchical flower-like structures

Fengjiao Chen,[a] Guowei Zhou,*[a] Hongjuan Chen,[a,b] Bin Sun[a] and Yan Zhang[a]

[a] Key Laboratory of Fine Chemicals in Universities of Shandong, School of Chemistry and Pharmaceutical Engineering, Qilu University of Technology, Jinan 250353, P. R. China

[b] School of Environmental Science and Engineering, Tianjin University, Tianjin 300072, P. R. China

E-mail: guoweizhou@hotmail.com (G. W. Zhou).

Chemicals. All the chemical reagents used in the experiments were of analytical grade without further purification. Poly(ethylene glycol)-*block*-poly(propylene glycol)-*block*-poly(ethylene glycol) (P123) was purchased from Aldrich. Acetic acid (HAc), tetrabutyl titanate (TBT) and other chemicals were all obtained from Tianjin Chemical Agent Company (China). Deionized water was used for all preparations.

Synthesis of flower-like titanate assembled by layered nanosheets. First, 1 g P123 was dissolved in 36.75 ml acetic acid, and kept stirring at 350 rpm for 2 h at 40 °C. Second, 1.0 ml TBT was added under stirring at rate of 500 rpm. The solution was kept under static conditions at 40 °C for varied time to form a uniform solution. Prolonged static times changed the color of the uniform solution from yellow to white, the viscosity increased and a colloidal solution was obtained. The colloidal solution was transferred into a teflon-lined autoclave and heated at 150 °C for 24 h under static conditions. Finally, the white solid products were collected by filtration, washed with ethanol, dried at 60 °C and calcined at 450 °C in a tube furnace for 5 h. Samples obtained without calcination, with calcination, and without adding P123 were respectively designated as FT-*x*, CFT-*x*, and WFT-*x*, where *x* is the static time.

Photocatalytic activity. The photodegradation of *p*-chlorophenol was carried out in an aqueous solution at room temperature under UV light irradiation. The photodegradation reaction was conducted in a cylindrical quartz reactor that had a water circulation facility at its outer wall. A 375 W high-pressure mercury lamp was used as the UV light source, and the distance between the reactant and light source was about 20 cm. In a typical experiment, 60 mg of the photocatalyst powders were

dispersed in 100 mL of *p*-chlorophenol solution (60 mg L^{-1}) with stirring. The suspension was stirred for 30 min in the dark to achieve adsorption−desorption equilibrium. The mixture was subsequently illuminated with the UV lamp and bubbled with oxygen at a constant flow rate. In order to determine the change in *p*-chlorophenol concentration during UV irradiation, 10 mL aliquots of the suspension were withdrawn at appropriate times from the reactor and centrifuged at 6000 rpm for 15 min at a characteristic wavelength (λ = 224 nm). According to the absorbance before and after illumination, the percent degradation of *p*-chlorophenol can be calculated.

Characterization. X-ray diffraction (XRD) patterns were recorded using a D8 advance diffractometer (Bruker Company) with Cu Kα radiation (30 kV, 30 mA, λ=0.15406 nm) and a step size of 0.02 from 5° to 70°. Transmission electron microscopy (TEM) studies were obtained on a JEM-2100 electron microscope with an acceleration voltage of 200 kV. Scanning electron microscopy (SEM) studies and selected area electron diffraction (SAED) were performed using a FEI Quanta 200 FEG microscope operating at an accelerating voltage of 30 kV. Fourier transformed infrared (FT-IR) spectra were collected on a Bruker Tensor 27 spectrometer with resolution and scan number of 4 cm^{-1} and 32, respectively. Samples were prepared using the standard KBr disk method and were measured at 400–400 cm^{-1}. The N_2 adsorption–desorption experiments were performed using a Micromeritics Tristar 3020 at 77 K. The surface area and pore size distribution were estimated via the Brunauer-Emmett-Teller (BET) and Barrett-Joyner-Halenda (BJH) methods based on

the adsorption isotherm.

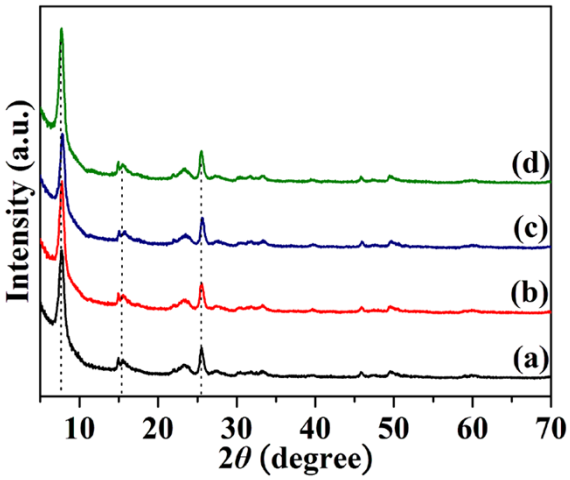

Fig. S1 XRD patterns of FT-1 (a), FT-2 (b), FT-48 (c), and FT-96 (d).

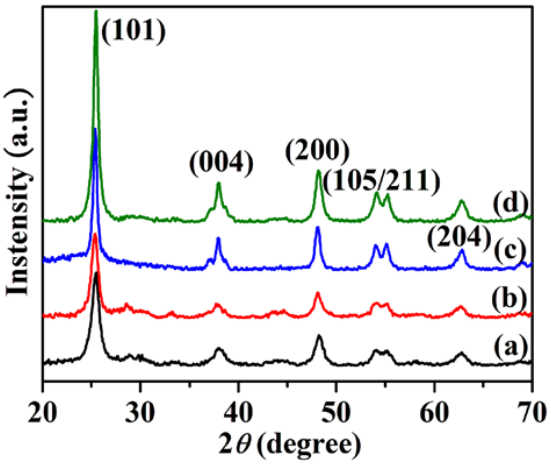

Fig. S2 XRD patterns of CFT-1 (a), CFT-2 (b), CFT-48 (c), and CFT-96 (d).

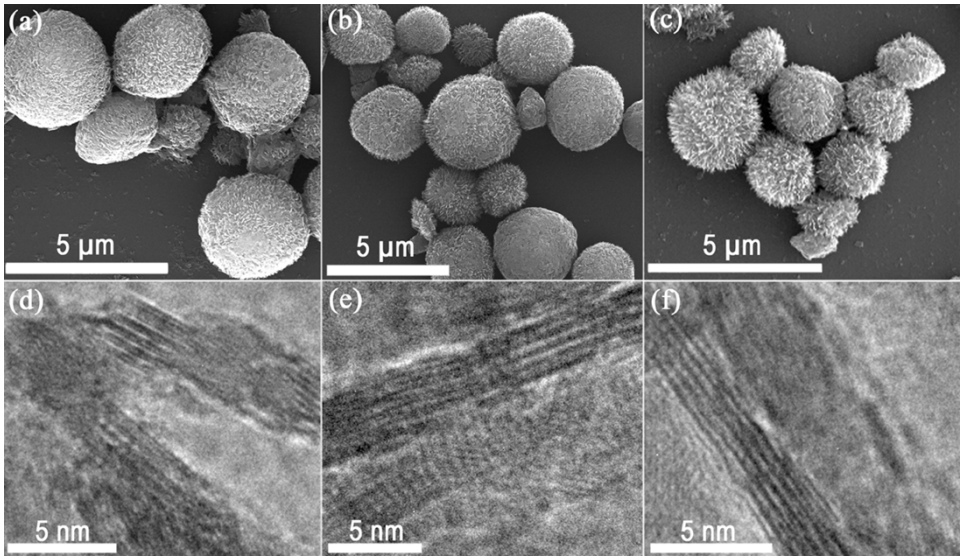

Fig. S3 SEM images of CFT-1 (a), CFT-2 (b), and CFT-48 (c); HRTEM images of CFT-1 (d), CFT-2 (e), and CFT-48 (f).

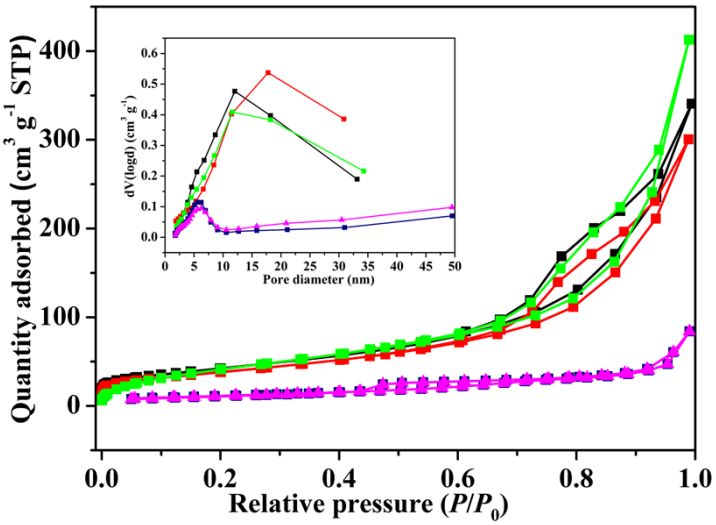

Fig. S4 N_2 adsorption-desorption isotherm curves and pore size distribution (inset) of CFT-2 (■), CFT-48 (■), CFT-96 (■), WFT-1 (■), and WFT-48 (▲).

Table S1 The surface areas and pore sizes of CFT-2, CFT-48, CFT-96, WFT-1, and WFT-48.

	CFT-2	CFT-48	CFT-96	WFT-1	WFT-48
S_{BET} (m^2 g^{-1})	142.9	145.7	131.4	41.0	41.3
Pore size (nm)	11.5	12.0	17.8	5.8	6.3

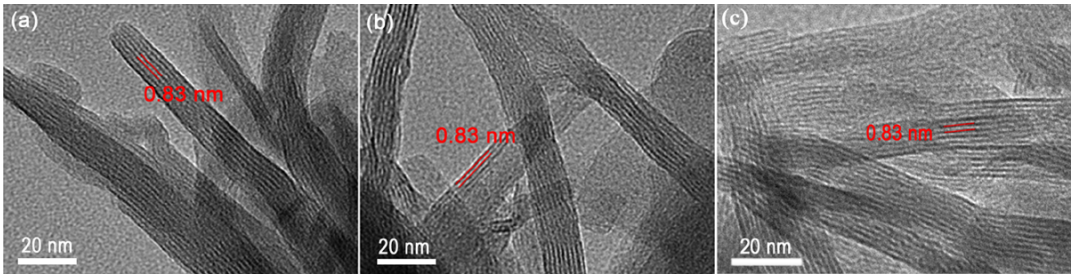

Fig. S5 HRTEM images of the obtained samples from different static time: FT-1 (a), FT-2 (b), and FT-48 (c).

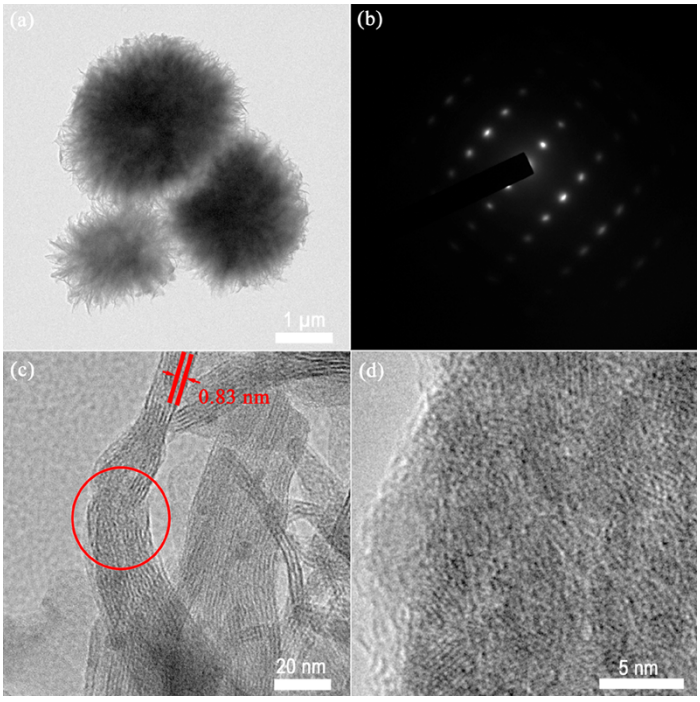

Fig. S6 TEM image (a) of WFT-1, SAED pattern (b) of small spindle-shaped particles in WFT-1, and HRTEM images of nanosheets at the beginning HRTEM testing process of WFT-1 (c) and at the end of testing process (d).

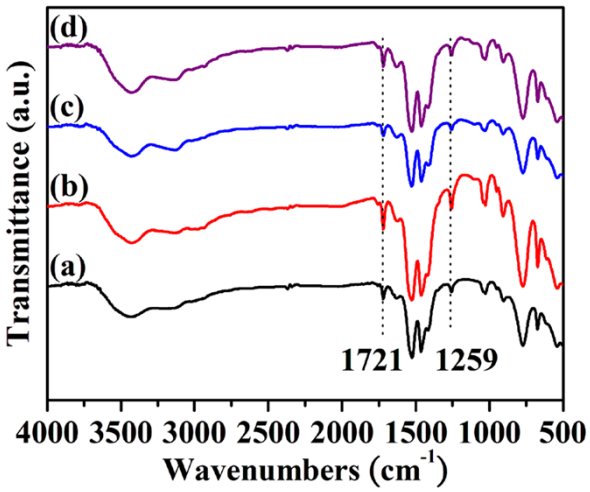

Fig. S7 FT-IR patterns of FT-1 (a), FT-2 (b), FT-48 (c), and FT-96 (d).

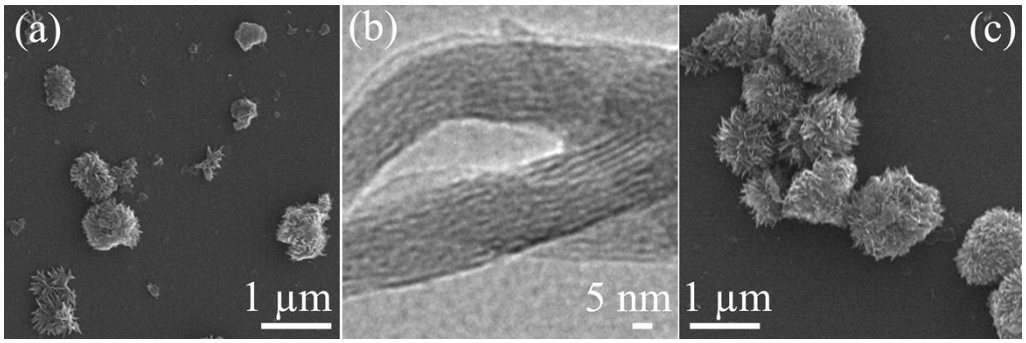

Fig. S8 SEM images of FT-0.08 (a) and FT-0.5 (c), HRTEM image of FT-0.08 (b).

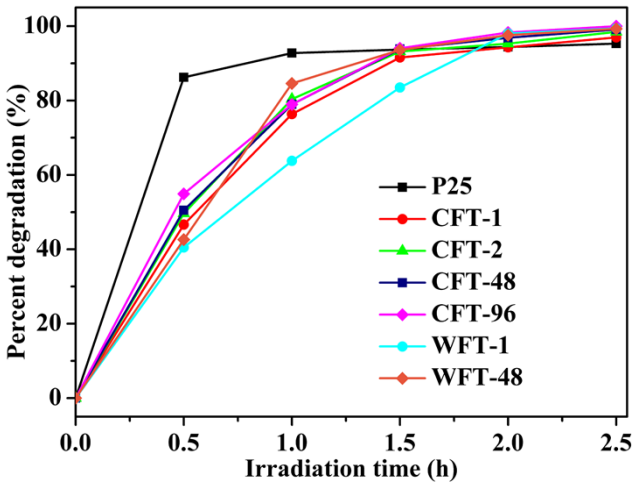

Fig. S9 Photocatalytic percent degradation of *p*-chlorophenol in the presence of CFT-1 as a function of UV light irradiation time (●), CFT-2 (▲), CFT-48 (■), CFT-96 (♦), WFT-1 (●), WFT-48 (♦), and P25 (■).